Journal of Magnetic Resonance 211 (2011) 207–216

Contents lists available at ScienceDirect

Journal of Magnetic Resonance

journal homepage: www.elsevier.com/locate/jmr

Complex molecular dynamics of $(CH_3NH_3)_5Bi_2Br_{11}$ (MAPBB) protons from NMR relaxation and second moment of NMR spectrum

L. Latanowicz [a,*], W. Medycki [b], R. Jakubas [c]

[a] Faculty of Biological Sciences, University of Zielona Góra, Szafrana 1, 65-516 Zielona Góra, Poland
[b] Institute of Molecular Physics, PAN, Smoluchowskiego 17, 60-179 Poznań, Poland
[c] Faculty of Chemistry, University of Wrocław, Joliot Curie 14, 50-383 Wrocław, Poland

ARTICLE INFO

Article history:
Received 16 February 2011
Revised 12 April 2011
Available online 7 June 2011

Keywords:
Molecular dynamics
Proton spin–lattice relaxation time
Proton second moment of the NMR line
Spectral densities
Complex motion
Schrödinger equation

ABSTRACT

Molecular dynamics of a polycrystalline sample of $(CH_3NH_3)_5Bi_2Br_{11}$ (MAPBB) is studied on the basis of the proton T_1 (55.2 MHz) relaxation time and the proton second moment of NMR line. The T_1 (55.2 MHz) was measured for temperatures from 20 K to 330 K, while the second moment M_2 for those from 40 K to 330 K. The proton spin pairs of the methyl and ammonium groups perform a complex stochastic motion being a resultant of four components characterised by the correlation times τ_3^T, τ_3^H, τ_2, and τ_{iso}, referring to the tunnelling and over the barrier jumps in a triple potential, jumps between two equilibrium sites and isotropic rotation. The theoretical expressions for the spectral densities in the cases of the complex motion considered were derived. For τ_3^H, τ_2, and τ_{iso} the Arrhenius temperature dependence was assumed, while for τ_3^T – the Schrödinger one. The correlation times τ_3^H for CH_3 and NH_3 groups differ, which indicates the uncorrelated motion of these groups. The stochastic tunnelling jumps are not present above the temperature T^{tun} at which the thermal energy is higher than the activation energy of jumps over the barrier attributed to the hindered rotation of the CH_3 and NH_3 groups. The T^{tun} temperature is 54.6 K for NH_3 group and 46.5 K for CH_3 group in MAPBB crystal. The tunnelling jumps of the methyl and ammonium protons are responsible for the flattening of T_1 temperature dependence at low temperatures. The isotropic tumbling is detectable only from the M_2 temperature dependence. The isotropic tumbling reduces the second moment to 4 G^2 which is the value of the intermolecular part of the second moment. The motion characterised by the correlation time τ_2 is well detectable from both T_1 and M_2 temperature dependences. This motion causes the appearance of T_1 minimum at 130 K and reduction of the second moment to the 7.7 G^2 value. The small tunnelling splitting ω_T of the same value for the methyl and ammonium groups was estimated as 226 MHz from the Haupt equation or 80 MHz from the corrected by us Haupt equation. These frequencies correspond to 0.93 μeV and 0.34 μeV tunnel splitting energy.

1. Introduction

Molecular-ionic halogenoantimonates(III) and halogenobismuthates(III) of the general formula $R_aM_bX_{3b+a}$ (where M = Sb, Bi and X = Cl, Br, I), containing organic cations in the crystal structure, have evoked much interest as they exhibit ferroelectric, ferroelastic and nonlinear optical properties [1–3]. Numerous structural studies have shown that these derivatives are characterised by a rich diversity of anionic structures. The type of anionic form in these complexes is clearly connected with the size and symmetry of the organic counter ions and their ability to form N–H···X hydrogen bonds [4–6]. It is interesting that the appearance of ferroelectricity in the $R_aM_bX_{3b+a}$ family of crystals is limited mainly to $M_2X_9^{3-}$ or $M_2X_{11}^{5-}$ anionic stoichiometry. For the compounds characterised by the chemical composition $R_3M_2X_9$, the polar properties were found in complexes where R stands for small alkylammonium cations like $[CH_3NH_3^+]$ [7], $[(CH_3)_2NH_2^+]$ [8] or $[(CH_3)_3NH^+]$ [9]. The compounds of the composition $R_5M_2X_{11}$ are rather rare. So far, only several examples of compounds crystallising with this chemical composition, containing methylammonium [10], pyridinium [11] and imidazolium [12] cations in the crystal structure have been found. All known $R_5M_2X_{11}$ complexes exhibit ferroelectric properties. The paraelectric–ferroelectric phase transitions found in the $R_5M_2X_{11}$ and $R_3M_2X_9$ subgroups were classified as of "order–disorder" type. The origin of the ferroelectricity was found to be related to the dynamics of dipolar organic cations [1,13].

$(CH_3NH_3)_5Bi_2Br_{11}$ (MAPBB) appeared to be the first example of crystals having isolated $(Bi_2Br_{11})^{-5}$ units in the crystal lattice [14]. It is built up of five types of methylammonium cations (MA) and isolated $(Bi_2Br_{11})^{-5}$ anions. MAPBB is found to undergo a ferroelectric phase transition of the *mmmFmm*2 type (from *Pcab* to *Pca*21 space group at 311.5 K). Dielectric dispersion [15] and

* Corresponding author.
E-mail address: jlat@amu.edu.pl (L. Latanowicz).

1090-7807/$ - see front matter © 2011 Elsevier Inc. All rights reserved.
doi:10.1016/j.jmr.2011.05.016

Raman scattering [16] studies have indicated the – order–disorder" mechanism of the phase transformation. The lowest temperature phase 4 transition is manifested by a nonlinear increase in spontaneous polarisation and dielectric anomaly in the vicinity of 77 K [17]. The molecular mechanism of the phase transition is based mainly on the single-crystal X-ray diffraction studies. In high temperature paraelectric phases (I) two of the five MA cations are ordered while the other three are disordered. The observed disorder consists of two equilibrium positions for each site between which the cations can jump. Through the phase transition at 311.5 K one MA cation becomes ordered, whereas the remaining two are still disordered over the ferroelectric phase (II). These two cations are believed to contribute to the phase transition mechanism (II → III) at about 77 K. Detailed mechanism of the transition from phase II to III is still unclear and the symmetry (space group) of the lowest temperature phase (III) is still unknown.

The methylammonium salts have been extensively investigated in connection with the appearance of various phase transitions including ferroelectric ones. The $(CH_3NH_3)^+$-cations below room temperature are believed to perform rotations around the C–N axes. Two kinds of such reorientations are considered to be possible. The first one is the correlated reorientation of the CH_3 and NH_3 groups in the cation i.e. all cations are equivalent and rotate as a whole around the C–N axes. Another kind of motion is the uncorrelated reorientation of the CH_3 and NH_3 groups. The information on this problem has been reported in papers based upon NMR relaxation and neutron quasielastic scattering methods [18–25]. The problem of the correlated/uncorrelated hindered rotations of CH_3 and NH_3 will be considered in our paper. The MA cation dynamics in ferroelectric phase of MAPBB has not been analysed by other methods yet.

The purpose of this work was to obtain comprehensive information about the methyl ammonium cations dynamics of MAPBB in a wide temperature regime, from measurements of the temperature dependence of the proton relaxation time T_1 (55.2 MHz) and the second moment of NMR line. The T_1 time was measured from 20 K to 330 K, while the second moment M_2 from 40 K to 330 K. The theoretical expressions for the spectral densities for the complex motion presented are derived. The tunnelling effects are analysed.

The vibrational levels of CH_3 and NH_3 groups are split with $E_T = \hbar\omega_T$ tunnel splitting energy. This tunnel splitting frequency ω_T imposes the spin splitting ω_i in the magnetic field. The values of ω_T can be estimated from the Haupt equation [26] or from the corrected Haupt equation proposed by us.

The complex motion of MAPBB protons from the melting point to the liquid nitrogen temperature (77 K) has been studied by proton spin–lattice relaxation times T_1 (90 MHz) [27]. The high temperature shallow minimum was visible in the T_1 (90 MHz) temperature dependence. The authors of Ref. [27] interpreted this minimum assuming the Dunn and McDowell theory [28] as due to C_3' reorientation of the whole cation about the C_3' axis making an angle of 13° with the C_3 axis of NH_3 and CH_3 groups. This motion can be compared with the motion above the liquid nitrogen temperature detected also by us. The motion identified separately by the $T_{1\rho}$ (B_1 = 10.7 Gs) method [27] as the 180° flip motion of the methylammonium cation can be compared with the motion identified by us on the basis of second moment reduction, at highest temperatures. Also previous T_1 (90 MHz) results helped us recognise the tunnel splitting frequency in the MAPBB.

2. Experimental

The crystals of pentakis(methylammonium) undecabromodibismuthate $[CH_3NH_3]_5$ $[Bi_2Br_{11}]$ (MAPBB) were obtained by the method described in Ref. [29]. The material was powdered and sealed in glass ampoules. ^{1}H NMR spin–lattice relaxation time (T_1) measurements were carried out as a function of temperature at 55.2 MHz, using Bruker SXP 4/100 pulsed spectrometer. Inversion recovery pulse sequence was used for the measurement of T_1. The temperature of the sample was varied from 293 to 20 K with the help of a continuous gas flow helium cryostat (CF1200 Oxford Instruments Cryosystem) and controlled to the accuracy of ±0.5 K. Slightly nonexponential decays of magnetisation were observed in the whole temperature range. The initial slopes of these decay plots were used to determine the spin–lattice relaxation time, T_1.

The second moment of the ^{1}H NMR line was calculated from a solid echo signal. Solid echo sequence [30] ($90^\circ_x - \tau - 90^\circ_y$) (with τ = 17 μs). The normalised line shape of the solid echo spectrum was identical to that of the FID spectrum. Therefore, the second moment can be determined on the basis of analysis of the solid echo shape [31]. The estimated average error on measured T_1 values is 5%, while the corresponding values for M_2 values are approximately 10%.

3. Results and discussion

3.1. Proton T_1 relaxation time

The present paper considers the proton dynamics in a wide temperature regime from 40 K up to the melting point. The temperature dependence of the proton relaxation time T_1 (55.2 MHz) for $(CH_3NH_3)_5Bi_2Br_{11}$ (MAPBB) is shown in Fig. 1a–c by open circles. Results of the earlier measurements [27] of proton T_1 of MAPBB performed at 90 MHz resonance frequency are shown also in Fig. 1b and c by triangles.

Two separate minima on T_1 (55.2 MHz) temperature dependence are visible. The temperature dependence of T_1 (55.2 MHz) suggests that the observed broad minimum (two less separated minima) of relaxation time T_1 near 50 K can be assigned to the classical C_3 hindered rotations of CH_3 and NH_3 groups, in the threefold potential. The relaxation time at minimum value equals $T_1^{\min} = \frac{\omega_i}{1.425C}$, where C is the relaxation constants and ω_i is the resonance frequency. The higher the value of C the shorter the relaxation time T_1^{min} is. The relaxation constant C is proportional to the R_{is}^{-6} (the distance between the protons to minus six powers). The smaller the value of R_{is}, the higher the value of C and the deeper the T_1 minimum. The H–H distance in CH_3 and NH_3 groups are 0.178 nm and 0.170 nm. Moreover the minimum with the lower activation energy is shifted to lower temperatures. We can see that the lower value T_1 minimum belongs to higher temperatures and the higher value T_1 minimum belongs to lower temperatures. The low temperature slope of these minimums indicates the lower activation energy of 2.64 kJ/mol. Therefore the two less separated minima of relaxation time T_1 near 50 K are caused by NH_3 motion at higher and CH_3 motion at lower temperatures. Dotted lines in Fig. 1a show contributions from the separate motions. The separate minima at about 50 K caused by the different temperature dependencies of the correlation time prove that the hindered rotation of CH_3 and NH_3 groups around C–N axis is uncorrelated. The shallow minimum in high temperatures (at about 130 K) suggests the additional motion of the whole methylammonium cation. There is also a small change in log T_1 vs $1/T$ dependence at the temperature of the transition from the ferroelectric to paraelectric phase T_{c1} = 311.5 K. The flattening of the T_1 temperature dependence in the lowest temperatures is characteristic for the presence of the tunnelling jumps through the threefold potential barrier [25,32–34]. In the lattice that can be described as almost rigid, the mechanisms that are normally neglected come into play. One of such mechanisms can be also relaxation via paramagnetic impurities,

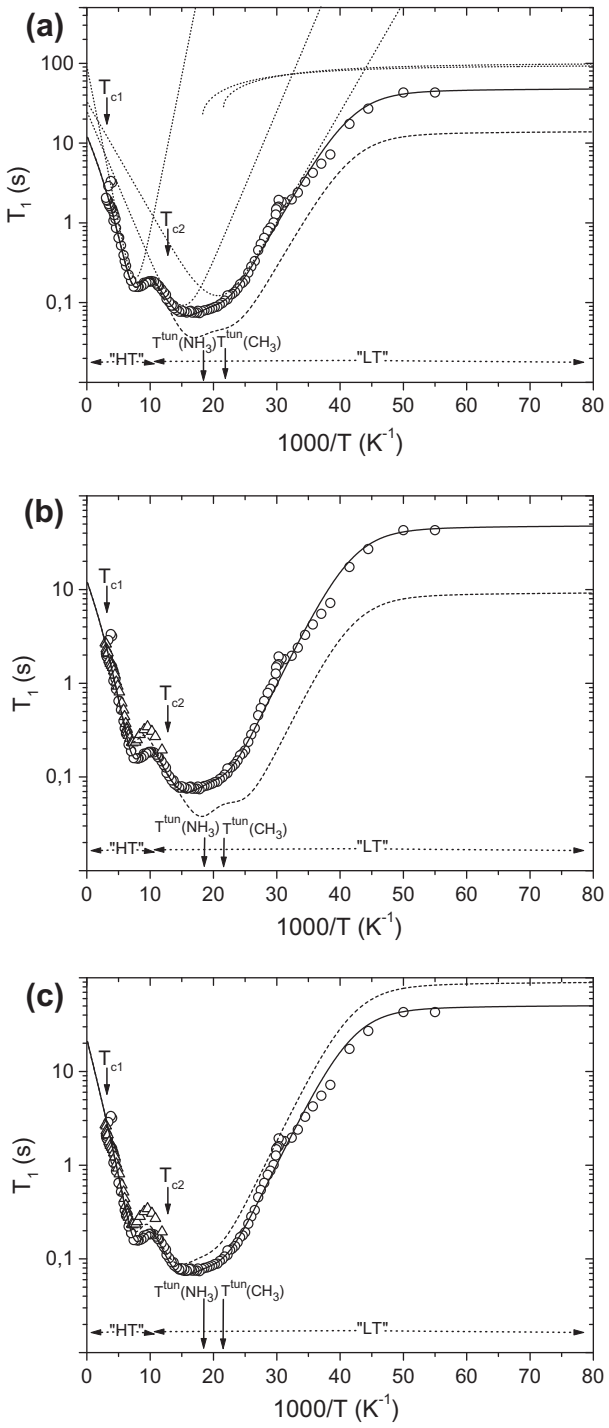

Fig. 1. Experimental data of the proton T_1 at 55.2 MHz (○) and 90 MHz (Δ). The solid line in (a–c) presents the fit T_1 (55.2 MHz) to the theoretical equations (see text) assuming Eq. (11) with ω_T = 226 MHz or Eq. (12) with ω_T = 80 MHz. The dotted lines in (a) show the separate contributions from the motions to this fit. The dashed line in (a) presents the same fit assuming ω_T = 0 MHz. The dashed lines in Fig 1b–1c presents the fit of the T_1 (90 MHz) experimental data to the theoretical equations assuming Eq. (11) with ω_T = 226 MHz (Fig. 1b) and Eq. (12) with ω_T = 80 MHz (Fig. 1c). The arrows show the T_{c1} (311.5 K) and T_{c2} (77 K) transitions and also T^{tun} temperatures. Unequal activation energies E_H of CH_3 and NH_3 separate the T^{tun} into two temperatures ($T^{tun}(NH_3)$ = 54.6 K, $T^{tun}(CH_3)$ = 46.5 K). The low and high temperature regimes are designed as "LT" and "HT".

whose T_1 is usually proportional to the square root of the resonance frequency [35]. Unfortunately we do not have access to measurements at two resonance frequencies. The reduction in T_1 with increasing temperature is attributed to the decrease in the electronic spin–lattice relaxation time with increasing temperature. The effect of the T_1 reduction with increasing temperature at low temperatures is not observed. T_1 is almost temperature independent. Such a behaviour of T_1 at the lowest temperatures has been observed not only by us but also recently in tetramethylammonium selenate [25] as well as in some methyl bearing compounds [32,33] The tunnelling jumps became dominant at low temperatures, when the probability of the Arrhenius over the barrier jumps is almost zero. It is well known in the literature that the tunnelling correlation times according to Müller-Warmuth et al. [36], Skinner–Trommsdorff [37] are weakly or Schrödinger [38] no temperature dependent, which is the reason for the low temperature flattening of the temperature dependence of relaxation time T_1. The tunnelling effects have to be present in the methyl, ammonium and methylammonium cations without any doubts. Therefore, we cannot ignore such an obvious stochastic motion (tunnelling jumps through the barrier) as a mechanism of the lowest temperatures T_1 relaxation. The relaxation via paramagnetic impurities can be neglected even in compounds as sensitive to impurities as sugars [39].

The values of spin–lattice relaxation time T_1 at the minimum at about 50 K longer than expected from the classical theory only (compare the solid and dashed lines in Fig 1a) reveal the tunnel splitting of XH_3 where X = C, N [25,26,32–34].

The fractions of molecules n_{v0} and $n_{v1,}$ in separate vibrational levels can be assumed to be Boltzmann fractions of molecules associated with average energies of the ground and first excited levels. Because the population of molecules in the second excited level is very low, it seems reasonable to assume that all molecules occupy two torsional levels ($n_{v0} + n_{v1} = 1$, $n_{v1}/n_{v0} = \exp(-E_{01}/RT)$). Therefore, the values of n_{v0}, n_{v1} are

$$n_{v0} = \frac{1}{\exp(-E_{01}/RT) + 1} \tag{1}$$

$$n_{v1} = \frac{\exp(-E_{01}/RT)}{\exp(-E_{01}/RT) + 1} \tag{2}$$

and the relaxation rate is

$$\frac{1}{T_1} = n_{v0}\left(\frac{1}{T_1}\right)_{v0} + n_{v1}\left(\frac{1}{T_1}\right)_{v1} \tag{3}$$

The $(1/T_1)_{v0}$, and $(1/T_1)_{v1}$ are the relaxation rates of the molecules in the ground and first excited vibrational states. The values of $(1/T_1)_{v0}$, and $(1/T_1)_{v1}$ are

$$\left(\frac{1}{T_1}\right)_{v0} = \left(\frac{1}{T_1}\right)_{v0}^{\text{intra}} + \left(\frac{1}{T_1}\right)_{v0}^{\text{inter}} \tag{4}$$

$$\left(\frac{1}{T_1}\right)_{v1} = \left(\frac{1}{T_1}\right)_{v1}^{\text{intra}} + \left(\frac{1}{T_1}\right)_{v1}^{\text{inter}} \tag{5}$$

where $(1/T_1)_{v0}^{\text{intra}}$, $(1/T_1)_{v1}^{\text{intra}}$, $(1/T_1)_{v0}^{\text{inter}}$, $(1/T_1)_{v1}^{\text{inter}}$ are the relaxation rates for the H–H dipolar interactions inside the methyl group (intra) and dipolar interactions between methyl group proton and out of methyl group proton (inter) with the spectral densities corresponding to the motions at these levels.

According to the classical mechanics, to overcome a potential barrier, the particles must have kinetic energy (thermal energy) greater than the height of the barrier. The correlation time for jumps over the potential equivalent barriers is

$$\tau_3^H = \tau_{03}^H \exp(E_H/RT) \tag{6}$$

where τ_{03}^H is the preexponential factor, $E_H = V_H - E_{v0}$ is the molar activation energy, V_H and E_{v0} are the potential barrier height and

the energy of the ground state vibrational level for the Avogadro number of particles.

According to quantum mechanics, the particles whose kinetic energy is lower than the barrier height can jump through a potential barrier (incoherent tunnelling, tunnelling correlation time, τ_3^T, characterises this motion). The stochastic molecular motions in the ground and first excited vibrational states do not have the same rates. Therefore, the correlation times τ_3^H, τ_3^T for separate $v0$ and $v1$ states have to be defined separately. Assuming that Eq. (6) defines the $(\tau_3^H)_{v0}$, the respective correlation times for $v1$ can be defined as

$$(\tau_3^H)_{v1} = \tau_{03}^H \exp[(E_H - E_{01})/RT] \tag{7}$$

$$\left(\frac{1}{(\tau_3^T)}\right)_{v1} = k'\left(\frac{1}{(\tau_3^T)}\right)_{v0} \tag{8}$$

where $E_{01} = E_{v1} - E_{v0}$ and $k' \gg 1$.

The value of $k' \gg 1$ indicates a faster rate of tunnelling in the first excited vibrational state than in the ground state. The value k' of about 30 has been established for the rate $(\tau_3^T)_{v1}$ of the proton transfer in the hydrogen bond [40,41].

The values $(1/T_1)_{v0}^{\text{inter}}$, $(1/T_1)_{v1}^{\text{inter}}$ are much smaller than the $(1/T_1)_{v0}^{\text{intra}}$, $(1/T_1)_{v1}^{\text{intra}}$ in the MAPBB crystal because of higher distances between the respective protons. Moreover the $(1/T_1)_{v1}^{\text{intra}}$ can be neglected because the population of the molecules at $v1$ is small (Fig. 2).

All protons of MAPBB are in the methyl or ammonium groups. Assuming that the reorientations of CH_3 and NH_3 groups about the C–N bond axis are independent of each other and that spin diffusion takes place, the resultant T_1 value can be expressed by

$$\frac{1}{T_{1v0}^{\text{intra}}} = \frac{1}{2}\left[\frac{1}{T_{1v0}^{\text{intra}}}(CH_3) + \frac{1}{T_{1v0}^{\text{intra}}}(NH_3)\right] \tag{9}$$

where $\frac{1}{T_{1v0}^{\text{intra}}}(CH_3, NH_3) = \frac{1}{3}\sum_{i=1}^{3}\sum_{s=1}^{3}\frac{1}{(T_{1ij}^{\text{intra}})_{v0}}$ is a sum of dipolar interacting proton pairs in the methyl or ammonium groups. If CH_3 and NH_3 reorientations were correlated, the correlation times of both groups would be the same.

Let's consider the T_1 temperature dependence in the low ("LT") temperature regime (Fig. 1). The tunnelling jumps are responsible for the flattening of the T_1 temperature dependence at low temperatures below about 20 K and the change in the low temperature slope minimum T_1 at about 30 K. The classical C_3 jumps are manifested as a wide T_1 minimum at about 50 K. The following two effects determine the T_1 temperature dependence in the "LT" regime:

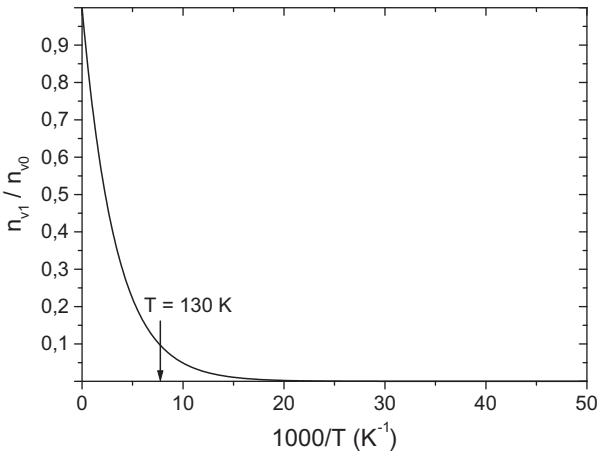

Fig. 2. The ratio n_{v1}/n_{v0} according to the Eqs. (1) and (2). The E_{01} was assumed 1.26 kJ/mol.

1. The splitting $\hbar\omega_T$ of the vibrational states of the methyl or ammonium group superimposes the Zeeman splitting of spin levels ω_i in a magnetic field. The tunnelling splitting $\hbar\omega_T$ of each vibrational level is driven by the symmetry of the XH_3 group, where X = C, N. The infinitesimally small number of molecules at the excited vibrational levels at low temperatures (below $1000/T = 15\ K^{-1}$) permits us to consider the ground vibrational state only. The symmetry conserving transitions ($\hbar\omega_i$ and $2\hbar\omega_i$) are forbidden by the spin selection rules. Therefore Haupt [26] has proposed to replace the angular NMR frequencies ω_i and $2\omega_i$ in the well-known BPP formula [42] with $\omega_i \pm \omega_T$ and $2\omega_i \pm \omega_T$ frequencies, respectively. Because of the tunnelling splitting of XH_3 group, the T_1 relaxation time does not fulfil the BPP equation at the minimum value (dashed line in Fig. 1a). When the values of ω_T are high in Gigahertz range then T_1 does not depend on the resonance frequency ω_i (~MHz).
2. The specific character of the T_1 temperature dependence is due to complex motion of methyl and ammonium groups in a triple potential, consisting of jumps over the barrier as well as tunnelling jumps through the barrier. The jumps over the barrier and the tunnelling jump although geometrically identical (C_3 reorientation) are described by the different probabilities and occur via different pathways: one pathway is over the barrier and the other one is through the barrier. Therefore the jumps over the barrier and tunnelling jumps are components of a complex motion.

The T_1 time becomes temperature independent at the lowest temperatures because the correlation time of tunnelling is not temperature dependent. The following explanation of this phenomenon can be presented. The expression for the tunnelling correlation time has been derived in Refs. [43] and [44]:

$$\tau_3^T = \tau_{03}^T e^{B\sqrt{E_H - C_pT}} \tag{10}$$

where E_H is the activation energy per 1 mol of particles, the value of B depends on the mass, m, of the tunnelling particle and on the width of the potential barrier, L, that is $B = \frac{2L}{\hbar}\sqrt{\frac{2m}{N_{Av}}}$. The magnitude of barrier width L in methyl and ammonium groups can be estimated as 0.722 Å and 0.642 Å [38]. Thus $B = 0.102\ [\sqrt{Joul}]^{-1}$ for CH_3 and $B = 0.091\ [\sqrt{Joul}]^{-1}$ for NH_3. The C_pT is the average thermal energy of 1 mol particles, C_p is the molar heat capacity and T is temperature in the Kelvin scale. The values of C_p are temperature dependent. The temperature dependence of C_p for MAPBB is known from Ref. [45].

The solution of the Schrödinger equation for the problem of tunnelling motion of particles through the potential barrier, gives explicitly the rate constant of tunnelling jumps (probability of tunnelling, coefficient of transparency of the barrier), that is $k_3^T = k_{03}^{(T)} e^{-\frac{2L}{\hbar}\sqrt{2m(U_0 - E)}}$, where E is the energy of the particle and U_0 is the potential barrier heights. The energy $N_{Av}E = C_pT + E_{v0}N_{Av}$ characterises the energy of the Avogadro number of particles, E_{v0} is the energy of the ground state vibrational level. $U_0N_{Av} = N_{Av}E_{v0} + E_H$ (in joules per mole) concerns the potential barrier per 1 mol of particles. Therefore the value under square root is $N_{Av}E_{v0} + E_H - C_pT - N_{Av}E_{v0} = E_H - C_pT$. When temperature increases, the values of C_pT became higher than E_H. The value of $\exp(-\sqrt{E_H - C_pT}) = 1$ for $E_H = C_pT^{tun}$. T^{tun} is the characteristic temperature above which the probability of tunnelling jumps has no real value because the expression under the square root becomes negative. Above the temperature of T^{tun} the probability of tunnelling jumps is zero.

The Schrödinger equation applied by us solves several problems [38,43,44,46–49]. We are able to explain why tunnelling jumps are detectable only at low temperatures up to a certain temperature. The tunnelling jumps begin at a temperature, at which the thermal

energy of the particle becomes lower than the activation energy ($C_pT \leqslant E_H$). The probability of tunnelling increases when $C_pT \to 0$. The tunnelling jumps are expected for the light atoms H, D hopping in hydrogen bonds or methyl groups. The particles are also reflected from the barrier (coefficient of reflection from the barrier, probability of reflection). Thus, the potential barrier is an obstacle for the de Broglie waves related to thermal energies of the particles. However, the particles' energy higher than the potential barrier height allows their hopping over the barrier (Arrhenius law). The over the barrier (classical) jumps can exist up to the 0 K, but the correlation time τ_3^H is very long at low temperatures. The dominating motion are tunnelling jumps characterised by the correlation time τ_3^T .

The flattening of the T_1 low temperatures dependence follows from the temperature dependence of the Schrödinger tunnelling correlation time. The Schrödinger tunnelling correlation time τ_3^T takes a constant value at a low temperatures where $C_pT \ll E_H$, ($\tau_3^T \approx \tau_{03}^T e^{B\sqrt{E_H}}$) and the Arrhenius correlation time is long at low temperatures and therefore the T_1 becomes a constant value.

The Haupt equation for the T_1 relaxation rate of a proton pair "is" distanced by R_{H-H} and belonging to the XH_3 group is a sum of the spectral densities [26]

$$\frac{1}{(T_{1is})_{t0}^{\text{intra}}}=\frac{9}{16}\left[J_{is}^1(\omega_i+\omega_T)+J_{is}^1(\omega_i-\omega_T)+J_{is}^2(2\omega_i+\omega_T)+J_{is}^2(2\omega_i-\omega_T)\right] \tag{11}$$

where ω_T is the tunnelling splitting of the ground vibrational level and ω_i is the angular resonance frequency.

The numerical factor in the Haupt equation has to be assumed to be twice as small as that in BPP because when $\omega_T = 0$, both theoretical expressions should give identical results. When the tunnelling splitting is high, ($\omega_T \gg \omega_i$), the $J_{is}^m(\omega_i \pm \omega_T) \approx J_{is}^m(\omega_T)$ (spectral density for high value of ω_T is not resonance frequency dependent), where $m = 1, 2$, while for very small tunnelling splittings $J_{is}^m(\omega_i \pm \omega_T) \approx J_{is}^m(\omega_i)$ (BPP equation). Estimating the ω_T on the basis of Eq. (11) we have to assume that the Haupt equation, written intuitively, is proper. According to the Haupt equation, the T_1 relaxation time at minimum is longer than expected from the BPP equation for $\omega_T > 3\omega_i$ only. For the tunnelling splitting $\omega_T < 3\omega_i$, T_1 is shorter than that expected from BPP theory. It seems impossible and it has been a source of our doubts regarding the Haupt equation. The solid line in Fig. 1b presents the best fit of the T_1 (55.2 MHz) while the dashed line of the T_1 (90 MHz) to the theoretical equation assuming the $\omega_T = 226$ MHz in Haupt equation (Eq. [11]).

As the T_1 relaxation times shorter than expected from the BPP formula seem unreliable, the following argumentation can be carried out. The tunnel splitting frequency (due to XH_3 group symmetry) imposes the spin splitting in the magnetic field. Thus we expect that the BPP equation should be replaced by the equation

$$\frac{1}{(T_{1is})_{t0}^{\text{intra}}}=\frac{9}{8}\left\{J_{is}^1(\omega_i+\omega_T)+J_{is}^2[2(\omega_i+\omega_T)]\right\} \tag{12}$$

Eq. (12) approximated for low values of $\omega_T \ll \omega_i$ gives the same values of T_1 as the BPP equation, while approximated to high values $\omega_T \gg \omega_i$ gives the T_1 values at the ω_T resonance frequency, which is independent of the resonance frequencies of the spectrometer. The illustration of the Eq. (12) is presented by dashed line in Fig. 1c. Generally, it seems that the Haupt equation for the T_1 relaxation of XH_3 groups in the presence of tunnelling splitting should be verified by theoreticians. The Haupt equation fits well the experimental data for $\omega_T \gg \omega_i$ [32–34,43,44] but this equation seems to be incorrect for low values of ω_T.

The number of the stochastic processes of methyl ammonium cation modulates the two spins dipolar interaction Hamiltonian independently of each other. This is the case of the complex motion. Each motion has its own correlation function described by different correlation time: $\tau_3^T - C_3$ tunnelling jumps, $\tau_3^H - C_3$ over the barrier jumps and $\tau_2 - C_2$ jumps between two equilibrium positions distanced by the angle Θ_2. The jump angle $\Theta_3 = 120°$ for proton–proton relaxation vector belonging to the methyl or ammonium group.

The correlation function and spectral density of the complex motion of R_{is} relaxation vector, undergoing three motions can be derived in a simple way [48]:

$$\begin{aligned}\langle F_{is}^m(t)F_{is}^{m*}(t+\tau)\rangle = K^m\gamma_i^2\gamma_s^2\hbar^2R_{is}^{-6}&\left[\cos^2\Theta_3+\sin^2\Theta_3\exp\left(-\frac{|\tau|}{\tau_3^H}\right)\right]\\ &\times\left[\cos^2\Theta_3+\sin^2\Theta_3\exp\left(-\frac{|\tau|}{\tau_3^T}\right)\right]\\ &\times\left[(1-S)+S\exp\left(-\frac{|\tau|}{\tau_2}\right)\right]\end{aligned} \tag{13}$$

and

$$\begin{aligned}J_{is}^m(\omega) = K^m\gamma_i^2\gamma_s^2\hbar^2R_{is}^{-6}&\left\{(1-S)\left[\cos^2\Theta_3\sin^2\Theta_3\right.\right.\\ &\times\left(\frac{2\tau_3^H}{1+(\omega\tau_3)^2}+\frac{2\tau_3^T}{1+(\omega\tau_T)^2}\right)+\sin^4\Theta_3\frac{2\tau_{3HT}}{1+(\omega\tau_{3HT})^2}\left.\right]\\ &+S\left[\cos^4\Theta_3\frac{2\tau_2}{1+(\omega\tau_2)^2}+\cos^2\Theta_3\right.\\ &\times\sin^2\Theta_3\left(\frac{2\tau_{3H2}}{1+(\omega\tau_{3H2})^2}+\frac{2\tau_{3T2}}{1+(\omega\tau_{3T2})^2}\right)\\ &\left.\left.+\sin^4\Theta_3\frac{2\tau_{3HT2}}{1+(\omega\tau_{3HT2})^2}\right]\right\}\end{aligned} \tag{14}$$

where $K^m = 4/5, 2/15, 8/15$ for $m = 0, 1, 2$ and $S = 0.75\sin^2\Theta_2$ [50]. Third motion this can also be a C_3' rotation. Then $S = \sin^2\Theta_3'$ [28,50]. The S value for $\Theta_2 = 90°$ is identical to that for $\Theta_3' = 120°$. Therefore, the twofold jumps with the value $\Theta_2 = 90°$ cannot be distinguishable from the C_3 jumps in triple potential.

The correlation time for jumps between two equilibrium sites over the potential barriers is

$$\tau_2 = \tau_{02}\exp(E_2/RT) \tag{15}$$

where τ_{02} is the preexponential factor and E_2 is the activation energy and the correlation times τ_3^H and τ_3^T are given by Eq. (6) and (10). Moreover, other symbols in Eq. (14) are

$$\frac{1}{\tau_{3HT}}=\frac{1}{\tau_3^T}+\frac{1}{\tau_3^H} \tag{16}$$

$$\frac{1}{\tau_{3H2}}=\frac{1}{\tau_3^H}+\frac{1}{\tau_2} \tag{17}$$

$$\frac{1}{\tau_{3T2}}=\frac{1}{\tau_3^T}+\frac{1}{\tau_2} \tag{18}$$

$$\frac{1}{\tau_{3HT2}}=\frac{1}{\tau_3^H}+\frac{1}{\tau_3^T}+\frac{1}{\tau_2} \tag{19}$$

The spectral density expressed by Eq. (14) can be well converted into a sum of the two parts – $[J_{is}^m(\omega)]_{LT}$ and $[J_{is}^m(\omega)]_{HT}$ where LT and HT refer to the low and high temperature regimes of T_1 dependence.

$$\begin{aligned}[J_{is}^m(\omega)]_{LT} = K_m\gamma_i^4\hbar^2R_{is}^{-6}&\left[\sin^2\Theta_3\cos^2\Theta_3\left(\frac{2\tau_3^H}{1+(\omega\tau_3^H)^2}+\frac{2\tau_3^T}{1+(\omega\tau_3^T)^2}\right)\right.\\ &\left.+\sin^4\Theta_3\left(\frac{2\tau_{3HT}}{1+(\omega\tau_{3HT})^2}\right)\right]\end{aligned} \tag{20}$$

and

$$[J_{is}^{m}(\omega)]_{HT} = K^{m}\gamma_i^2\gamma_s^2\hbar^2 R_{is}^{-6} S\cos^2\Theta_3 \frac{2\tau_2}{1+(\omega\tau_2)^2} \quad (21)$$

The tunnelling jumps (τ_3^T correlation time) are not present in the high temperature regime, where the $\frac{2\tau_2}{1+(\omega\tau_2)^2}$ function achieves a maximum. The term $\cos^2\Theta_3 = \cos^2 120^0 = \frac{1}{4}$ in Eq. (21) represents the "memory" of the faster C_3 motion and it is usually called the "order parameter". The order parameter is the reason why the high temperature minimum of T_1 at 130 K is so high value. We have to remember that jumps between two sites are manifested at higher temperatures therefore it has to be slower than C_3 motion. That the T_1 relaxation time minimum corresponding to the slowest component motion is shallower than the minimum T_1 associated with such a motion in the absence of the faster motions has been shown in papers [51–57]. According to the approach to the tunnelling and jumps over the barrier of protons in triple potential known from literature, these motions are not treated as components of a complex motion [58]. The tunnelling correlation time is treated as a correction to the classical correlation time. Such an approach does not allow analysis of the entire temperature course of the T_1 relaxation time with the contributions coming from the other components of the complex motion.

By inserting Eq. (20) and (21) to Eq. (11) or Eq. (12), the following expression can be obtained for R_{is} vector belonging to each XH_3 group.

$$\frac{1}{(T_{1is})_{v0}^{\text{intra}}} = \left(\frac{1}{(T_{1is})_{v0}^{\text{intra}}}\right)_{LT} + \left(\frac{1}{(T_{1is})_{v0}^{\text{intra}}}\right)_{HT} \quad (22)$$

Eq. (22) should be inserted to Eq. (9) to obtain the whole temperature dependence of T_1 of MAPBB cation in the presence of a complex motion of methylammonium cation.

The fitted parameters in Eq. (22) are τ_3^T, τ_3^H, τ_2, Θ_2, E_H, E_2 and ω_T.

The best fits of the temperature dependencies of T_1 (55.2 MHz) and T_1 (90 MHz) to Eqs. (11) and (12) with the spectral density given in Eq. (14) are given by the solid lines in Fig. 1b and c. As we can see, both theoretical equations fit very well the experimental data T_1 (55.2 MHz). The greatest difference in the fitted parameters is in the ω_T values obtained. The fitted value of ω_T equals 226 MHz according to Eq. (11) and 80 MHz according to Eq. (12). These values correspond to the 0.93 μeV and 0.34 μeV energies of tunnelling splitting. The fit of the theoretical dependence given in Eq. (12) to experimental data can be performed without any assumptions concerning ω_T (Fig. 1c), but in the Haupt equation (Eq. (11)) we have to assume that the spectral densities of in the "LT" and "HT" temperature regimes were calculated for different ω_T frequencies. When we want to correlate the present experimental results at 55.2 MHz (circles) with previous results at 90 MHz (triangles) we have to assume in Eq. (11) the frequency ω_T = 226 MHz in the "LT" temperature regime and the frequency ω_T = 0 MHz for the "HT" temperature regime. The theoretical dependence T_1 (ω_i = 90 MHz, ω_T = 226 MHz) is situated below the T_1 (ω_i = 55.2 MHz, ω_T = 226 MHz) theoretical dependence in the "LT" temperature regime according to Eq. (11) (dashed line in Fig. 1b). Eq. (12) does not create such problems in T_1 temperature dependences. The dashed line in Fig. 1c is positioned above the solid line drawn according to Eq. (12). Also the fit of the whole temperature dependence was performed at the same frequencies ω_T. Therefore, the obtained value of ω_T of 80 MHz, seems to be more reliable than ω_T = 226 MHz. obtained from the Haupt equation.

The highest temperature shallow T_1 minimum at about 130 K is assigned to the jumps of the methylammonium cation between two positions distanced by the angle Θ_2 in the crystal lattice. The tunnelling jumps cease above T^{tun} temperature [43,44,46–49,59]. Therefore in the "HT" temperature regime the complex motion is a superposition of two classical motions of types C_3 and jumps between two sites (Eq. (21)). Both CH_3 and NH_3 groups of the methylammonium cation undergo conformational jumps between two equilibrium sites with the same frequency, therefore with the same correlation time τ_2 Assuming the proton–proton distance R_{is} in CH_3 and NH_3 groups as 0.178 nm and 0.170 nm, respectively, we can fit the experimental data to Eq. (9) with Eqs. (12) and (21) assuming the Θ_2 angle as 90°. For the angle Θ_2 = 90° the reduction of spectral density of C_2 motion goes through maximum ($S = 0.75\sin^2 90°$ in Eq. (21)), similarly as for the Θ_3 = 120° ($S = \sin^2 120°$ in Eq. (21) [28,50]). However, according to the authors of Ref. [27] the complex motion was concluded to be a composition of C_3 and C_3' hindered rotations. Both kinds of motion are equally possible, and their distinction from the high temperature T_1 minimum seems impossible. The best fit of T_1 (55.2 MHz) to Eq. (22) with Eqs. (9), (11), (12), (20), and (21) and respective frequencies $\omega = (\omega_i \pm 226)$ MHz and $\omega = (2\omega_i \pm 226)$ MHz (Eq. (11)) or $\omega = (\omega_i + 80)$ MHz and $\omega = 2(\omega_i + 80)$ MHz (Eq. (12)) is presented by solid line in Fig. 1a–c. The best fit parameters are listed in Table 1. The two values of T_{tun} follow from different activation energies E_H for the classical C_3 motion of CH_3 and NH_3 groups. These temperatures T_{tun} are 54.6 K for NH_3 group and 46.5 K for CH_3 group in MAPBB crystal. Individual contributions to T_1 from the separate motions are plotted in Fig. 1a by dotted lines. The tunnelling correlation time τ_3^T was not detected previously, because the measurements were performed only above liquid nitrogen temperature [27].

3.2. Proton second moment of NMR line

The second moment for the rigid lattice of a dipolar NMR line (in magnetic field units) M_2^{rigid} can be calculated assuming the Van Vleck theory [60]. When N is the number of interacting nuclei, then M_2^{rigid} is given by the averaged sum of the N dipolar interactions according to the formula

$$M_2^{rigid} = \frac{9}{20}\gamma_i^2\hbar^2\frac{1}{N}\sum_{i=1}^{N}\sum_{s=1}^{N}R_{is}^{-6} \quad (23)$$

The calculated proton rigid lattice second moment, M_2^{rigid}, for $(CH_3NH_3)_5Bi_2Br_{11}$ protons on the basis of the known structural data [14] is 31.1G^2. This value of M_2^{rigid} corresponds to the sum

$$M_2^{rigid} = M_2^{rigid}(\text{intra}) + M_2^{rigid}(\text{inter}) \quad (24)$$

where

$$M_2^{rigid}(\text{intra}) = \frac{1}{2}\left[M_2^{rigid}(CH_3) + M_2^{rigid}(NH_3)\right] \quad (25)$$

Assuming the proton–proton distances of 0.178 nm and 0.170 nm in CH_3 and NH_3 groups, respectively, $M_2^{rigid}(CH_3) = 22.5G^2$ and $M_2^{rigid}(NH_3) = 29.7G^2$. Therefore, the total M_2^{rigid}(intra) = 26.1G^2 and M_2^{rigid}(inter) = 5G^2.

Table 1
The motional parameters of protons in MAPBB.

	CH_3	NH_3
τ_{03}^H (s)	1.5×10^{-12}	1.5×10^{-12}
τ_{03}^T (s)	5.5×10^{-7}	5.5×10^{-7}
τ_{02} (s)	1.8×10^{-12}	1.8×10^{-12}
τ_0^{iso} (s)	3×10^{-12}	3×10^{-12}
E_H (kJ/mol)	2.64	3.6
E_2 (kJ/mol)	7.54	7.54
E_{iso} (kJ/mol)	33.5	33.5
ω_T (MHz)		
Eq. (11)	226	226
Eq. (12)	80	80
T^{tun} (K)	46.5	54.6

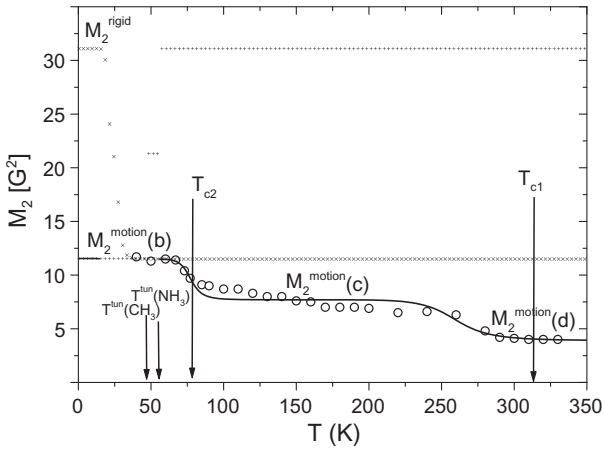

Fig. 3. Experimental proton M_2 (○). Solid line presents the fit of the data to Eq. (28), crosses curve to Eq. (30) and *x* curve to Eq. (31). The plateau $M_2^{motion}(b)$ arises from C_3 motions – classical and tunnelling jumps of CH_3 and NH_3 groups, the plateaus $M_2^{motion}(c)$ and $M_2^{motion}(d)$ are caused by the two sites jumps and isotropic motion of the methylammonium cation. The plateau $M_2^{motion}(d)$ indicates the intermolecular part of the second moment. The arrows show the ferroelectric to paraelectric phase, T_{c1} (311.5 K) and T_{c2} (77 K), transitions and also T^{tun} temperatures.

The experimental data of the proton second moment of NMR line, M_2, for $(CH_3NH_3)_5Bi_2Br_{11}$ are shown in Fig. 3 by open circles. The M_2 value of the MAPBB protons measured at about 50 K is close to 11.5 G^2, which is not the rigid lattice second moment value. It is nearly a few times lower than M_2^{rigid}. Unfortunately, the measurements of the second moment are not performed below the 40 K. The second moment undergoes two reductions ΔM_2 above 50 K: one at about 70 K and the other one at about 260 K. The reduction at ~70 K can be well correlated with the T_1 (55.2 MHz) minimum at about 130 K.

The motion responsible for the reduction ΔM_2 at the higher temperatures, at about 260 K, is undetectable on the T_1 temperature dependence. The motional parameters, probably of isotropic tumbling of cations, can be estimated from this reduction ΔM_2 of the second moment at 260 K.

It is well known that the second moment is sensitive to the stochastic motion. As proposed by Powles and Gutowsky [61], the statistical nature of motion permits the application of the correlation function method. The correlation function corresponds to the spectral density

$$M_{2is} = \frac{3}{4}\gamma^2\hbar^2 I(I+1)\int_{-\delta\nu}^{+\delta\nu} J_{is}^0(\nu)d\nu \tag{26}$$

where

$$J_{is}^0(\nu) = \int_{-\infty}^{+\infty} < F_{is}^0(t)F_{is}^0 * (t+\tau)\exp(i2\pi\tau)d\tau \tag{27}$$

where $\delta\nu$ is the NMR linewidth in frequency units, and ν is the Fourier frequency of the molecular motion.

As follows from the Powles and Gutowsky method, each reduction in the second moment appears when the frequency of the motion, which is characterised by the correlation time τ, is comparable to the NMR linewidth in frequency units ($(1/\tau_c) \approx 2\pi\delta\nu$). The maximum reduction in the second moment, M_2^{motion}, occurs at temperatures at which all the molecules reorient fast enough ($\tau_c \ll 1/(\gamma\sqrt{M_2^{rigid}})$) to reduce the line broadening [46,62–64].

The temperature dependence of the second moment due to complex motion consisting of four component motions (classical and tunnelling jumps of the CH_3 and NH_3 protons in the triple potential, jumps between two sites and isotropic motion of the methylammonium cation protons) can be calculated by the method presented in Ref. [46,62–64]

$$\begin{aligned} M_2 = {} & M_2^{rig} - \Delta M_2(a) - \Delta M_2(b) - \Delta M_2(c) - \Delta M_2(d) \\ & + \frac{1}{2}\Delta M_2(a)\left[\frac{2}{\pi}\tan^{-1}(\gamma_i\tau_3^T(CH_3)\sqrt{M_2}) + \frac{2}{\pi}\tan^{-1}(\gamma_i\tau_3^T(NH_3)\sqrt{M_2})\right] \\ & + \frac{1}{2}\Delta M_2(b)\left[\frac{2}{\pi}\tan^{-1}(\gamma_i\tau_3^H(CH_3)\sqrt{M_2}) + \frac{2}{\pi}\tan^{-1}(\gamma_i\tau_3^H(NH_3)\sqrt{M_2})\right] \\ & + \Delta M_2(c)\frac{2}{\pi}\tan^{-1}(\gamma_i\tau_2\sqrt{M_2}) + \Delta M_2(d)\frac{2}{\pi}\tan^{-1}(\gamma_i\tau_{iso}\sqrt{M_2}) \end{aligned} \tag{28}$$

where $\Delta M_2^{motion}(a)$, $\Delta M_2^{motion}(b)$, $\Delta M_2^{motion}(c)$, $\Delta M_2^{motion}(d)$ are reductions of M_2 caused by the separate motions characterised by the correlation times τ_3^T τ_3^H, τ_2 and τ_{iso}. The correlation time for isotropic tumbling equals

$$\tau_{iso} = \tau_0^{iso}\exp(E_{iso}/RT) \tag{29}$$

where τ_0^{iso} is the preexponential factor and E_{iso} is the activation energy.

Eq. (28) reduces to simpler form for the C_3 tunnelling jumps only ($\tau_3^H \to \infty$, $\tau_2 \to \infty$, $\tau_{iso} \to \infty$):

$$\begin{aligned} M_2 = {} & M_2^{rig} - \Delta M_2(a) + \frac{1}{2}\Delta M_2(a)\frac{2}{\pi}[\tan^{-1}(\gamma_i\tau_3^T(CH_3)\sqrt{M_2}) \\ & + \tan^{-1}(\gamma_i\tau_3^T(NH_3)\sqrt{M_2})] \end{aligned} \tag{30}$$

Eq. (28) is reduced to a simpler form for the C_3 classical jumps only ($\tau_3^T \to \infty$, $\tau_2 \to \infty$, $\tau_{iso} \to \infty$)

$$\begin{aligned} M_2 = {} & M_2^{rig} - \Delta M_2(b) + \frac{1}{2}\Delta M_2(b) \\ & \times \frac{2}{\pi}\left[\tan^{-1}(\gamma_i\tau_3^H(CH_3)\sqrt{M_2}) + \tan^{-1}(\gamma_i\tau_3^H(NH_3)\sqrt{M_2})\right] \end{aligned} \tag{31}$$

The best fits of the experimental data to Eqs. (28), (30) and (31) are presented by solid line crosses and *x* curves in Fig. 3.

It is known that the second moment values M_2 for the methyl bearing solids at liquid helium temperatures do not reach the value predicted for the rigid molecule. The second moment can be a few times lower than that calculated for the rigid structure [65,66]. This effect is due to stochastic tunnelling jumps. The tunnelling jumps reduce the M_2^{rigid} to the value $M_2^{motion}(a)$. The T_1 temperature measurements indicate that the tunnelling jumps are performed in the methyl and ammonium groups of MAPBB. The tunnelling correlation time τ_3^T is not temperature dependent at low temperatures ($\tau_3^T \approx \tau_{03}^T e^{B\sqrt{E_H}}$) at which the thermal energy of particles is much lower than the activation energy of the classical C_3 motion, E_H. The value of the second moment, $M_2^{motion}(a)$ reduced due to tunnelling jumps is expected theoretically at the temperature 0 K. The $\Delta M_2^{motion}(a) = \Delta M_2^{intra}(\tau_3^T) = 19.6\ G^2$ in the presented case (solid line and crosses curve near 0 K in Fig. 3). Tunnelling jumps reduce M_2 up to the T^{tun} temperature only. The tunnelling jumps cease above T^{tun} temperature at which $C_pT^{tun} = E_H$ [38,43,44,46–49,59]. The T^{tun} temperature equals 46.5 K for CH_3 and 54.6 K for the NH_3 group as follows from the T_1 measurements.

The second reduction of M_2^{rigid} to the value $M_2^{motion}(b)$ is caused by the classical C_3 jumps of CH_3 and NH_3 groups. This reduction $\Delta M_2^{motion}(b)$ begins about 20 K (see *x* curve in Fig. 3), when also the tunnelling jumps cause reduction in the second moment. Therefore, between 20 K and T^{tun} temperature, the second moment is reduced by two stochastic motions that are the classical and tunnelling jumps in the triple potential. This is only a theoretical prediction, supported by the τ_{03}^T and E_H activation parameters obtained from the T_1 temperature dependence, because we do not have the measurements of the second moment below 40 K. Because $\Delta M_2^{motion}(b) = \Delta M_2^{motion}(a)$ the reduced value of the second

moment $M_2^{motion}(b)$ equals 11.5 G^2 above T^{tun} temperature. The temperature regime between 20 K and 54.6 K can be treated as the intermediate temperature regime where both motions C_3 tunnelling and classical jumps influence the second moment M_2 values. We not show the temperature dependence of the second moment between these temperatures. The situation would be clearer when the tunnelling jumps would cease ($\tau_3^T \to \infty$) before the second moment reduction caused by the motion characterised by the correlation time τ_3^H.

If the C_3 motion is faster than the jumps between two sites and isotropic motion (the tunnelling motion is not present above the temperature 54.6 K), the reduction of the second moment is expected as $\Delta M_2(b) = \sin^2\Theta_3 M_2^{rigid}(\text{intra})$, where $\Theta_3 = 120°$ [46,62]. The fitted value $\Delta M_2(b) = 19.6\ G^2$ is in a very good agreement with the expected value. The $\Delta M_2(b)$ reflects the "true" reduction of the second moment. The other ones, $\Delta M_2(c)$, $\Delta M_2(d)$ are influenced by the "memory" (order parameters) of the faster motion reduction [63]. These order parameters take values lower than one. The value of the plateau $M_2^{motion}(c) = 7.7\ G^2$ corresponds to the second moment reduction $\Delta M_2(c) = 3.8\ G^2$. This reduction is due to the jumps between two equilibrium sites of the methylammonium cation characterised by the correlation time τ_2. It has been shown that the relaxation constant C calculated from the minimum of T_1 at 130 K and the fitted value of $\Delta M_2(c)$ are interrelated as:

$$C = \frac{2}{3}\gamma^2 \Delta M_2(c) \tag{32}$$

Therefore, the relaxation constant C corresponding to 3.8 G^2 is 18.1×10^8 s^2. Such a value of the relaxation constant was obtained from the T_1 high temperature minimum at 130 K.

The next reduction of the second moment $\Delta M_2(d) = 3.8\ G^2$ to the value of $M_2^{motion}(d) = 4.0\ G^2$ is probably due to the isotropic motion. This highest temperature reduction is visible only on the M_2 temperature dependence and does not correspond to any minimum of T_1. If the isotropic motion appeared as a single motion on the temperature scale, it would reduce the $M_2^{rigid}(\text{intra})$ to zero value. This value 4.0 G^2 corresponds, in the experimental error limit, to the $M_2^{rigid}(\text{inter})$ calculated as 5 G^2. It is interesting to note that the second moment reduction caused by isotropic tumbling happens just before the second order phase transition T_{c1} = 311.5 K. The best fit parameters τ_0^{iso} and E_{iso} are listed in Table 1. The motion identified by us as the isotropic motion was identified also on the basis of the $T_{1\rho}$ method as the 180° flip motion of the methylammonium cation. This motion has been predicted but not analysed by the authors of Ref. [27].

The best fit of Eq. (28) to the experimental data is presented in Fig. 3 by the solid line. The fitted parameters are $\Delta M_2^{\text{intra}}(b)$, $\Delta M_2^{\text{intra}}(c)$, $\Delta M_2^{\text{intra}}(d)$, E_{iso}, τ_0^{iso}. The other parameters were assumed from Table 1.

The values of the correlation times determine the order of the reductions in the second moment. The first reduction, due to τ_3^T appear at 0 K, the second one, due to τ_3^H begins at 20 K and the third and fourth reductions are due to τ_2 and τ_{iso} and take place above T^{tun} temperature.

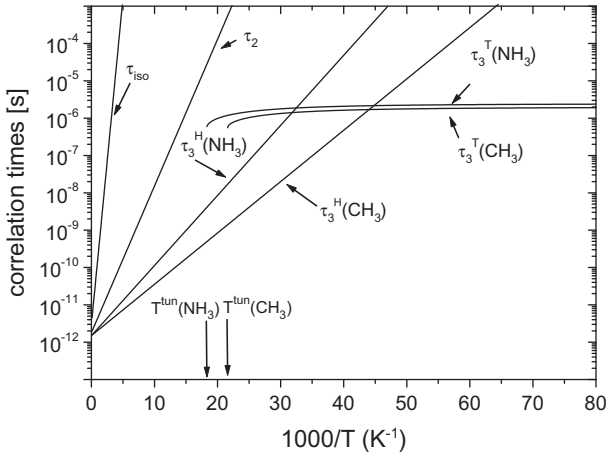

Fig. 4. Proton correlation times of C_3 tunnelling $\tau_3^T(CH_3)$, $\tau_3^T(NH_3)$, (Eq. (10)), and classical over the barrier jumps $\tau_3^H(CH_3)$, $\tau_3^H(NH_3)$, (Eq. (6)) of methyl and ammonium groups, of classical jumps between two sites of methylammonium cation τ_2 (Eq. (15)), and of isotropic rotation τ_{iso} (Eq. (29)), of the methylammonium cation as a function of 1000/T (K^{-1}). The motion parameters used to plots are taken from Table 1. The arrows show the T^{tun} temperatures.

3.3. Correlation times

The temperature dependences of the correlation times τ_3^H, τ_3^T, τ_2, τ_{iso} determined on the basis of the best fit parameters listed in Table 1 and Eqs. (6), (10), (15), and (29) are presented in Fig. 4. The τ_3^H at low temperatures is very long, therefore the dominant correlation time is τ_3^T. As follows from Eq. (10), the correlation time τ_3^T takes a constant value at low temperatures where $C_pT < E_H$ ($\tau_3^T \approx \tau_{03}^T e^{B\sqrt{E_H}}$). The τ_3^T correlation time exists up to the T_{tun} temperature only.

The activation energies E_H for CH_3 and NH_3 groups are different (Table 1) and therefore two different temperature dependences of τ_3^H. Therefore the classical motion C_3 of methyl and ammonium groups can be identified as an uncorrelated motion. Also two different values of E_H imply that temperature dependences of τ_3^T for CH_3 and NH_3 are different.

The correlation times τ_2 and τ_{iso} have the same activation energies and preexponential factors for protons from both CH_3 as well NH_3 groups. The motional parameters of τ_{iso} were obtained from the M_2 temperature dependence only.

4. Conclusions

The monomethylammonium protons in $(CH_3CN_3)_5Bi_2Br_{11}$ (MAPBB), polycrystalline material, undergoes a complex motion composed of four components. The tunnelling jumps (τ_3^T correlation time) are responsible for the temperature independent behaviour of T_1 at lowest temperatures and reduction in M_2 to the value of 11.5 G^2 at 0 K. The temperature of zero Kelvin is predicted theoretically on the basis knowledge of the Schrödinger tunnelling correlation time (from T_1 measurements). We do not have access to measurements of second moment at such low temperatures. The classical hindered C_3 rotation (τ_3^H correlation time) of methyl ($\tau_3^H(CH_3)$) and ammonium ($\tau_3^H(NH_3)$) groups is responsible for two T_1 (55.2 MHz) minima at about 50 K and for the plateau of M_2 equal 11.5 G^2 at about 50 K. The C_3 hindered rotation of CH_3 and NH_3 is not correlated. The correlation times of both groups differs by the activation energy.

The jumps between two equilibrium sites distanced at 90° of methylammonium cation (τ_2 correlation time), cause a shallow T_1 (55.2 MHz) minimum at a temperature about 130 K and the reduction in the second moment down to the plateau value equal 7.7 G^2.

The fourth one motion is that of isotropic motion of whole cation (τ_{iso} correlation time). The isotropic tumbling is detectable only on the M_2 temperature dependence. The isotropic motion reduces the second moment to 4.0 G^2 which is the value of the intermolecular part of the second moment. This reduction happen just before the temperature of the phase transition T_c = 311.5 K.

The small tunnelling splitting ω_T of the methyl and ammonium groups was estimated as 226 MHz from the Haupt equation or 80 MHz from the Haupt equation corrected by us. These frequencies

correspond to 0.93 μeV and 0.34 μeV tunnel splitting energy. Both small values of the tunnel splitting energy are lower than the experimental error in the neutron scattering measurements.

References

[1] L. Sobczyk, R. Jakubas, J. Zaleski, Self-assembly of Sb(III) and Bi(III) halo-coordinated octahedra in salts of organic cations. Structure, properties and phase transitions, Polish J. Chem. 71 (1997) 265–300 (and references cited therein).

[2] G. Xu, Y. Li, W. Zhou, G. Wang, X. Long, L. Cai, M. Wang, G. Guo, J. Huang, G. Bator, R. Jakubas, A ferroelectric inorganic–organic hybrid based on NLO-phore stilbazolium, J. Mater. Chem. 19 (2009) 2179–2183.

[3] W. Bi, N. Leblanc, N. Mercier, P. Auban-Senzier, C. Pasquier, Thermally induced Bi(III) lone pair stereoactivity: ferroelectric phase transition and semiconducting properties of (MV)BiBr5 (MV = methylviologen), Chem. Mater. 21 (2009) 4099–4101.

[4] M. Hall, M. Nunn, M.J. Begley, D.B. Sowerby, Nonahalogenodiantimon(III)ates; their preparation and the crystal structures of $[Hpy]_3[Sb_2Cl_9]$, $[NMe_4]_3[Sb_2Br_9]$, and $[NMe_4]_3[Sb_2Br_3Cl_6]$, J. Chem. Soc., Dalton Trans. (1986) 1231–1238.

[5] M. Nunn, A.J. Blake, M.J. Begley, D.B. Sowerby, Preparation and structures of two anionic antimony (III) mixed halides, Hpy $[SbBr_2Cl_2]$ and $[Hpy]_8[Sb_4Br_{12}Cl_8]$, Polyhedron 17 (1998) 4213–4217.

[6] H. Ishihara, K. Yamada, T. Okuda, A. Weiss, The structures of M2X93−(M = Bi; X = Cl, Br) ions determined by rietveld analysis of X-ray powder diffraction data, Bull. Chem. Soc. Jpn. 66 (1993) 380–383.

[7] M. Iwata, M. Eguchi, Y. Ishibashi, S. Sasaki, H. Shimizu, T. Kawai, S. Shimanuki, Phase transition in $(CH_3NH_3)3Bi_2Br_9$, J. Phys. Soc. Jpn. 62 (1993) 3315–3326.

[8] J. Zaleski, Cz. Pawlaczyk, R. Jakubas, H.-G. Unruh, Structure and dynamic dielectric behaviour of ferroelectric $[NH_2(CH_3)_2]_3Sb_2Br_9$ (DMABA), J. Phys. Condens. Matter 12 (2000) 7509–7521.

[9] M. Bujak, J. Zaleski, High temperature ferro-paraelectric phase transition in TMACA studied by X-ray diffraction method, Cryst. Eng. 4 (2001) 241–252.

[10] P. Carpentier, J. Lefebvre, R. Jakubas, Structure of pentakis(methylammonium) undecachlorodibismuthate(III), $[NH_3(CH_3)]_5Bi_2Cl_{11}$, at 130 K and mechanism of the phase transitions, Acta Crystallogr. B51 (1995) 167–174.

[11] J. Jóźków, R. Jakubas, G. Bator, A. Pietraszko, Ferroelectric properties of $(C_5H_5NH)_5Bi_2Br_{11}$, J. Chem. Phys. 114 (2001) 7239–7246.

[12] A. Piecha, A. Białońska, R. Jakubas, Structure and ferroelectric properties of $[C_3N_2H_5]_5[Bi_2Br_{11}]$, J. Phys. Condens. Matter 20 (2008) 325224–325233.

[13] P. Carpentier, P. Zielinski, J. Lefebvre, R. Jakubas, Phenomenological analysis of the phase transitions sequence in the ferroelectric crystal $(CH_3NH_3)_5Bi_2Cl_{11}$ (PMACB), Z. Phys. B: Condens. Matter 102 (1997) 403–414.

[14] J. Matuszewski, R. Jakubas, L. Sobczyk, T. Głowiak, Structure of pentakis(methylammonium) undecabromodibismuthate, Acta Cyst. C46 (1990) 1385–1388.

[15] C. Pawlaczyk, K. Planta, C. Bruch, J. Stephen, H.-G. Unruh, Dielectric dispersions in pentakis methyl ammonium bismuthate single crystals. I. $(CH_3NH_3)_5Bi_2Br_{11}$, J. Phys.: Condens. Matter 4 (1992) 2687–2694.

[16] R. Jakubas, L. Sobczyk, J. Lefebvre, A new ferroelectric crystal: $(CH_3NH_3)_5Bi_2Cl_{11}$, Ferroelectrics 100 (1990) 143–149.

[17] J. Mroz, R. Jakubas, Ferroelectricity in $(CH_3NH_3)_5Bi_2Br_{11}$ crystals, Solid State Commun. 72 (1989) 813–816.

[18] S. Albert, H.S. Gutowsky, J.A. Ripmeester, On a T_1 and T_1 (study of molecular motion and phase transitions in the tetramethylammonium halides, J. Chem. Phys. 56 (1972) 3672–3676.

[19] Y. Furukawa, H. Kiriyama, R. Ikeda, Molecular motion in methylammonium hexahalotellurates(IV) as studied by means of the pulsed nuclear magnetic resonance, Bull. Chem. Soc. Jpn. 54 (1981) 103–108.

[20] H. Ishida, R. Ikeda, D. Nakamura, Motion of methylammonium ions in solid $CH_3NH_3NO_3$ and CH_3NH_3SCN studied by ^1H NMR, Bull. Chem. Soc. Jpn. 55 (1982) 3116–3118.

[21] R. Jakubas, G. Bator, W. Medycki, N. Piślewski, R. Decressain, J. Lefebvre, P. François, Dilatometric, dielectric and NMR studies of structural phase transitions of the $(CH_3NH_3)_3Bi_2Cl_9$ (MACB) crystals, J. Mol. Struct. 385 (1996) 145–151.

[22] R. Jakubas, J.A. Janik, J. Krawczyk, J. Mayer, T. Stanek, O. Steinsvoll, Neutron quasielastic scattering by $(CH_3NH_3)_5Bi_2C_{11}$, Physica B 241 (243) (1998) 481–483.

[23] W. Medycki, NMR study of monomethylammonium cation in $(CH_3NH_3)_5Bi_2Cl_{11}$ ferroelectric polycrystal, Solid State NMR 13 (1999) 213–218.

[24] W. Medycki, Classical and quantum molecular dynamics of cation in $(CH_3NH_3)_3Sb_2Br_9$ polycrystal as studied by ^1H NMR, Solid State NMR 14 (1999) 37–143.

[25] K.J. Mallikarjunaiah, K.C. Paramita, K.P. Ramesh, R. Damle, Study of molecular reorientation and quantum rotational tunnelling in tatramethylammonium selenate by ^1H NMR, Solid State NMR 32 (2007) 11–15.

[26] J. Haupt, Einfluß von quanteneffecten der methylgruppenrotation auf die kernrelaxation in festkörpern, Z. Naturforsh. 26 (a) (1971) 1578–1589.

[27] L. Piekara - Sady, R. Jakubas, N. Pislewski, Molecular motions in a novel ferroelectric crystal $(CH_3NH_3)_5Bi_2Br_{11}$ studied by NMR, Solid State Commun. 72 (1989) 585–587.

[28] M.B. Dunn, C.A. McDowell, An NMR study of molecular motion in solid trimethylaminegallane, Mol. Phys. 24 (1972) 969–978.

[29] R. Jakubas, A new ferroelectric compound: $(CH_3NH_3)_5Bi_2Br_{11}$, Solid State Commun. 69 (1989) 267–269.

[30] J.G. Powles, P. Mansfield, Double-pulse nuclear-resonance transients in solids, Phys. Lett. 2 (1962) 58–59.

[31] P. Mansfield, Multiple-pulse nuclear magnetic resonance transients in solids, Phys. Rev. 137 (1965) 961–974.

[32] F. Köksal, E. Rössler, Spin–lattice relaxation by tunnelling motions of methyl groups in some organic compounds, Solid State Commun. 44 (1982) 233–235.

[33] F. Köksal, E. Rössler, H. Sillescu, Spin–lattice relaxation by tunneling motions of methyl groups in four acetates, J. Phys: Solid State 15 (1982) 5821–5827.

[34] K. Morimoto, Small tunneling splitting of methyl-group and $T_{1\rho}$ of protons in pentamethylbenzene, J. Phys. Soc. Jpn. 39 (1975) 1413–1414.

[35] A. Abragam, The Principles of Nuclear Magnetism, Oxford University Press, 1961 (Chapter 9).

[36] W. Müller-Warmuth, R. Schüler, M. Prager, A. Kollmar, Rotational tunnelling in methylpyridines as studied by NMR relaxation and inelastic neutron scattering, J. Chem. Phys. 69 (1978) 2382–2392.

[37] J.L. Skinner, H.P. Trommsdorff, Proton transfer in benzoic acid crystals: a chemical spin-boson problem. Theoretical analysis of nuclear magnetic resonance, neutron scattering, and optical experiments, J. Chem. Phys. 89 (1988) 897–907.

[38] L. Latanowicz, P. Filipek, Tunneling molecular dynamics in the light of the corpuscular-wave dualism theory, J. Phys. Chem. A 111 (2007) 7695–7702.

[39] E.C. Reynhardt, An NMR, DSC and X-ray investigation of the disaccharides sucrose, maltose and lactose, Mol. Phys. 69 (1990) 1083–1097.

[40] D.F. Brougham, A.J. Horsewill, R.I. Jenkinson, Proton transfer dynamics in the hydrogen bond: a direct measurement of the incoherent tunnelling rate by NMR and the quantum-to-classical transition, Chem. Phys. Lett. 272 (1997) 272.

[41] A.J. Horsewill, D.F. Brougham, R.I. Jenkinson, C.J. McGloin, H.P. Trommsdorff, M.R. Johnson, The quantum dynamics of proton transfer in the hydrogen bond, Ber. Bunsenges Phys. Chem. 102 (1998) 317.

[42] N. Bloemebergen, E.M. Purcell, R.V. Pound, Relaxation effects in nuclear magnetic resonance absorption, Phys. Rev. 73 (1948) 679–712.

[43] L. Latanowicz, Proton spin–lattice relaxation of tunnelling methyl groups: calculation of the time dependent correlation functions, J. Phys. Chem. A 108 (2004) 11172–11182.

[44] L. Latanowicz, NMR relaxation study of methyl groups in solids from low to high temperatures, Con. Mag. Reson. A 27 (2005) 38–53.

[45] A. Jeżowski, R. Poprawski, J. Mróz, Thermal conductivity anomalies in $(CH_3NH_3)_5Bi_2Br_{11}$ crystals, J. Korean Phys. Soc. 32 (1998) S210–S211.

[46] L. Latanowicz, W. Medycki, R. Jakubas, The effect of low-temperature dynamics of the dimethylammonium group in $[(CH_3)_2NH_2]_3Sb_2Cl_9$ on proton spin–lattice relaxation and narrowing of the proton NMR, J. Phys. Chem. A 109 (2005) 3097–3104.

[47] L. Latanowicz, W. Medycki, Application of Schrödinger equation to study the tunnelling dynamics of proton transfer in the hydrogen bond of 2,5-dinitrobenzoic acid. Proton T_1, $T_{1\rho}$ and deuteron T_1 relaxation methods, J. Phys. Chem. A 111 (2007) 1351–1357.

[48] L. Latanowicz, W. Medycki, R. Jakubas, Complex methyl groups dynamics in $[(CH_3)_4P]_3SB_2Br_9$ (PBA) from low to high temperatures by proton spin–lattice relaxation and narrowing of proton NMR spectrum, Solid State NMR 36 (2009) 144–150.

[49] L. Latanowicz, Complex methyl group and hydrogen-bonded proton motions in terms of the Arrhenius and Schrödinger equations, Solid State NMR 34 (2008) 93–104.

[50] L. Latanowicz, E.C. Reynhardt, Nuclear spin–lattice relaxation and complex motions in polycrystalline solids, Mol. Phys. 90 (1997) 107–118.

[51] D.E. Woessner, Spin relaxation processes in a two-proton system undergoing anisotropic reorientation, J. Chem. Phys. 36 (1962) 1–4.

[52] D.E. Woessner, Nuclear magnetic dipole–dipole relaxation in molecules with internal motion, J. Chem. Phys. 42 (1965) 1855–1859.

[53] D. Wallach, Effect of internal rotation on angular correlation functions, J. Chem. Phys. 47 (1967) 5258–5269.

[54] D.E. Woessner, B.S. Snowden, G.H. Meyer, Nuclear spin–lattice relaxation in axially symmetric ellipsoids with internal motion, J. Chem. Phys. 50 (1969) 719–721.

[55] D.E. Woessner, B.S. Snowden, Magnetic relaxation under hindered rotation in fluids, Adv. Mol. Relax. Process. 3 (1972) 181–197.

[56] L. Latanowicz, Z. Gdaniec, Effect of the frequency of intramolecular motions on the NMR relaxation in liquid state temperature regime, Mol. Phys. 107 (2009) 1563–1576.

[57] L. Latanowicz, Z. Gdaniec, Nuclear spin–lattice relaxation and complex motion of macromolecules in solution, Mol. Phys. 109 (2011) 853–861.

[58] A.J. Horsewill, Quantum tunnelling aspects of methyl group rotation studied by NMR, Prog. NMR Spectrosc. 35 (1999) 359–389.

[59] L. Latanowicz, E.C. Reynhardt, J. Boguszyńska, Complex dynamics of proton and deuteron transfer in double hydrogen bond of benzoic acid isotopes, J. Mol. Struct. (Teochem) 710 (2004) 111–117.

[60] J.H. Van Vleck, The dipolar broadening of magnetic resonance lines in crystals, Phys. Rev. 74 (1948) 1168–1183.

[61] J.G. Powles, H.S. Gutowsky, Proton magnetic resonance of the CH3 group. III. Reorientation mechanism in solids, J. Chem. Phys. 23 (1955) 1692–1699.

[62] L. Latanowicz, E.R. Andrew, E.C. Reynhardt, Second moment of an NMR spectrum of a solid narrowed by molecular groups in potential wells with nonequivalent sites, J. Magn. Reson. A 107 (1994) 194–202.

[63] L. Latanowicz, E.C. Reynhardt, Dipolar NMR spectrum of a solid narrowed by a complex molecular motion, J. Magn. Reson. A 121 (1996) 23–32.
[64] E.C. Reynhardt, L. Latanowicz, ^{1}H and ^{2}H NMR relaxation in hydrogen-bonded solids due to a complex motion: classical jumps over the barrier and incoherent tunneling, J. Magn. Reson. 130 (1998) 195–208.
[65] E.R. Andrew, R.G. Eades, Z.M. Elsaffar, J.P. Llewellyn, Proton magnetic resonance at low temperatures of molecular solids containing CH_3 groups, Bull. Amp. 9 (1960) 379.
[66] P.S. Allen, Proton second moment of an isolated tunnelling methyl group, J. Chem. Phys. 48 (1968) 3031–3036.